This article has been accepted for publication in IEEE Sensors Journal. This is the author's version which has not been fully edited and content may change prior to final publication. Citation information: DOI 10.1109/JSEN.2025.3567576



# 5G Tiny-ML AI-based IoT eNose system for Hazardous Odour Detection and Classification

Rafael Fayos-Jordan, Mohammad Alselek, Mohamed Khadmaoui-Bichouna, Jaume Segura-Garcia, Jose M. Alcaraz-Calero* *Senior Member, IEEE, Qi Wang*

***Abstract*—More than 2 million people have died in the world in 2019 exposed to hazard substances. In this context, it is of paramount importance to deliver effective systems to help minimizing such number of dead. The usage of advanced technologies, such as artificial intelligence (AI) and the Internet of Things (IoT), plays a critical role in the detection of hazardous substances within Industry 4.0. The combination of these technologies enhance the efficiency and accuracy of monitoring harmful materials, improving safety standards and operational processes in industrial environments. AI can be used to analyse vast amounts of data for identifying patterns and predicting potential hazards, while IoT connects various devices and sensors to ensure real-time tracking and prompt responses to risks. This technological synergy is essential for modern industries aiming to create safer and more automated systems. In this work, we propose a 5G AI-IoT e-Nose system for the real-time detection and classification of 5 hazardous odours. The proposed AI model is very lightweight and it is affordable for our IoT micro controller unit. The system has been validated in laboratory conditions, but has the advantage and potential impact to be effective in any scenario.**

***Index Terms*—5G, AI, IoT, Hazardous substances, classification.**

## I. Introduction

An electronic nose (e-nose) is a device that mimics the olfactory system of humans and other animals to detect and identify odours or volatile compounds. It utilizes sensors and pattern recognition algorithms to analyse the chemical composition of a sample and generate a corresponding odour profile. The basic components of an electronic nose typically include an array of chemical sensors, signal processing units, and pattern recognition algorithms. The sensor array consists of different types of chemical sensors, such as metal oxide semiconductors, conducting polymers, or quartz crystal microbalances, which respond to various volatile compounds by changing their electrical properties. When an odour or gas sample is introduced to the electronic nose, the sensors in the array detect and measure the changes in their electrical signals. These signals are then processed and analysed by the device's software or pattern recognition algorithms. By comparing the obtained pattern with a pre-established database of known odour profiles, the e-nose can be used to identify and classify the sample based on its odour characteristics [1], [2].

One advantage of electronic noses is their ability to detect odours that are imperceptible to the human nose. They can also provide fast and objective results, eliminating the subjectivity and variability associated with human sensory perception. Furthermore, electronic noses can be used in environments that are hazardous or inaccessible to humans, ensuring safety and efficiency in various industries. However, there are some limitations to electronic noses. They may have difficulties distinguishing between complex mixtures of odours or detecting low concentrations of certain compounds. Calibration and regular maintenance are also necessary to ensure accuracy and reliability. Additionally, while electronic noses can detect and classify odours, they do not provide information about the identity or structure of the compounds responsible for the odour.

Despite these limitations, electronic noses continue to evolve and find new applications. Ongoing research focuses on improving sensor technologies, enhancing pattern recognition algorithms, and developing portable and miniaturized e-nose devices. With further advancements, electronic noses have the potential to revolutionize odour analysis, quality control, and diagnostics in various industries.

It is estimated that approximately 2 million people worldwide died in 2019 due to exposure to hazardous chemicals [3]. Just in the European part of the World Health Organisation (WHO), where 209 million hazardous substances were produced in 2017, this figure amounts to 269,500 deaths. These figures are often underestimated, as morbidity is calculated and recorded only for certain chemicals, ignoring many others. These concerning data highlight the severity and importance of implementing rigorous safety measures in the handling and production of these substances.

In the work environment, according to the European Agency for Safety and Health at Work (EU-OSHA), 16% of workers handle substances hazardous to health and 22% are exposed to toxic fumes or vapours for at least a quarter of their working time [4]. These exposures are not just limited to the chemical industry; they also cover a wide range of sectors that use these agents in their daily operations, such as cleaning products, fuels and other chemicals. This reality implies that virtually every industry is involved in the handling of hazardous substances to some degree. The impact of these exposures is

R. Fayos-Jordan, M. Alselek, Qi Wang are with the School of Computing, Engineering and Physics, University of the West of Scotland, Scotland, PA1 2BE, United Kingdom, e-mail: rafael.fayos@uws.ac.uk

J. Segura-Garcia is with the ETSE - Universitat de Valencia, Valencia, 46100, Spain, email: jaume.segura@uv.es

Jose M. Alcaraz-Calero is with the School of Computer Science and Digital Technologies, Aston University, Birmingham, B4 7ET, United Kingdom, e-mail: j.alcarazcalero@aston.ac.uk

M. Khadmaoui-Bichouna is with Tech Lead, London, England. e-mail:m.khadmaoui@exus.ai

Manuscript received September 15, 2024; revised October XX, XXX.

This article has been accepted for publication in IEEE Sensors Journal. This is the author's version which has not been fully edited and content may change prior to final publication. Citation information: DOI 10.1109/JSEN.2025.3567576



significant. According to the Occupational Safety and Health Administration's (OSHA) "Severe Injury Reports", 80.79% of serious accidents involving hazardous substances are due to inhalation of these substances [5]. This figure highlights the critical importance of implementing adequate safety measures to protect workers from the risks associated with inhaling hazardous chemicals. In addition to serious accidents, there are also a considerable number of minor accidents that do not require hospitalisation but can have cumulative effects on workers' health in the long term.

The need for strict policies and continuous monitoring is evident to mitigate the risks associated with exposure to hazardous chemicals at the workplace. Industries must take further steps to reduce the incidence of accidents and protect workers' health. Substances posing a greater risk to workers include liquids that emit toxic vapours, such as gasoline, isopropyl alcohol, ammonia and bleach. The impact on exposure is explained in detail in the next section. These volatile compounds are of particular concern because of their widespread use in various industries and their ability to release vapours harmful to health. Inhalation can lead to a variety of respiratory disorders, ranging from irritation and breathing difficulties to chronic diseases of the respiratory system. In extreme situations, exposure to high concentrations of these vapours can be fatal.

Human-involved accidents are mainly due to the lack of a cost-effective, wearable solution for real-time detection of exposure and inhalation of hazardous substances, allowing for their mass deployment in the work environment. Current systems lack these features, complicating the task of alerting workers and safety officers to spills or leaks of hazardous substances within a short time frame. These are often based on sensors for specific gases placed on the ceiling, away from the source of the hazard, or require laboratory analysis to identify the substance and take appropriate action, or are very expensive portable solutions [6]–[8].

Our main contribution consists of the design, implementation and validation of a Tiny-ML real-time IoT wearable device for the identification of hazardous substances in work environments. This device, based on artificial intelligence, is designed to alert workers and safety managers with the aim of reducing fatalities and injuries.

This manuscript provides the following innovations with respect the state of the art

- Nobel Dataset of Hazard Substances. Obtaining odour records of hazardous substances with nanotube sensor arrays is one of the first aims of this work.
- New Tiny-ML AI Algorithm for the detection of substances using electronic odorimeters. In our work, we also propose a Neural Network with 4 layers for the classification of hazardous substance odour records.
- Integrated validated Architecture for performing AI-driven substance detection. This work also presents an implementation of the AI model in a ESP32 IoT device.
- System model prototype demonstrated in a relevant environment. After training and implementing the AI model into the wearable device, the system will be validated and evaluated in terms of power consumption and performance.

After this introductory section, the paper is organised as follows: In Section 2, an interdisciplinary analysis of the repercussions of human exposure to hazardous substances within our system is conducted. After that, in section 3, a brief state-of-the-art is presented. In section 4, the architecture of the 5G AI-IoT system is described. In section 5, the AI system is detailed, defining the dataset, describing the AI model, and establishing the training pipeline. Section 6 describes the training results with some discussion. Then, section 7 explains the inference results, presenting some power consumption measurements. Section 8 describes the whole system validation with applications. Finally, section 9 summarises the main conclusions of this work.

## II. Impact in Human Health related to the Exposure to Hazard Substances

This section provides an explanation of the different impacts in human health associated with the exposure to the different hazard substances addressed in this research work.

Gasoline is a colourless to slightly amber liquid, mainly used as a vehicle fuel and solvent. It has an odour threshold of 0.25 ppm, indicating its ability to be detected at low concentrations. Gasoline is highly flammable and explosive. Skin contact can cause irritation and burns, and may cause eye damage. Inhalation of its vapours can irritate the nose, throat and lungs, leading to coughing and shortness of breath. Prolonged exposure can induce several adverse symptoms, including headache, nausea, weakness, dizziness, blurred vision, irregular heartbeat, lack of coordination, light-headedness, and fainting. In extreme cases, exposure to high levels of gasoline can be fatal. According to the American Conference of Governmental Industrial Hygienists (ACGIH), exposure to a threshold limit value (TLV) above 300 ppm on average during an 8-hour work shift is not recommended, and a short-term exposure limit (STEL) of 500 ppm. [18], [19].

Isopropyl alcohol is a colourless liquid with a strong characteristic odour detectable at 22 ppm and above. It is one of the most widely used substances in industry, playing a role in the production of cosmetics, pharmaceuticals, cleaners, antifreeze and many other chemicals. Contact with isopropyl alcohol can cause irritation and burns to the skin and eyes. Repeated exposure may result in skin rashes, itching, dryness and redness. Inhalation of isopropyl alcohol vapours can irritate the nose and throat, and repeated exposure to high concentrations can lead to adverse symptoms such as headache, dizziness, confusion, loss of coordination, unconsciousness and even death. To minimise the risks associated with exposure to isopropyl alcohol, a maximum TLV of 200 ppm averaged over an 8-hour workshift and a STEL of 400 ppm are recommended [20].

Ammonia is a colourless gas that commonly occurs in aqueous solutions. It has a pungent and irritating odour, detectable at concentrations of 5 ppm and above. This compound is widely used in various industries, including the manufacture of fertilisers, refrigerants, textiles, detergents and pesticides,

This article has been accepted for publication in IEEE Sensors Journal. This is the author's version which has not been fully edited and content may change prior to final publication. Citation information: DOI 10.1109/JSEN.2025.3567576



TABLE I
SUMMARY TABLE FOR THE SOA IN OUR 5G AI-IOT ENOSE

| | Sensor Array | Sensor Type | Harm.Substs | Mult. Substs. | Nr.Substs./ /Nr.Character. | IoT Dev. | Op. Env. | Wireless Connect. | DSP process. | AI Tech. |
|---|---|---|---|---|---|---|---|---|---|---|
| [9] | Multiple | MOx[1] | Y/Bio (COVID) | N | 1 / 615 | N | In lab | N | Y (HEPA filt) | ML/DNN |
| [10] | Multiple (6) | MOx[1] | N (Wine quality) | N | 1 / 4 | Y | In situ | N | Y (filt) | ML |
| [11] | Multiple (7) | MOx[1] | N (Essent. Oils) | Y | 1 / 6 | Y | In situ | N | Y (filt&Norm) | ML |
| [12] | Multiple (16) | MOx[1] & QMB[2] | N (diff. odours) | Y | 76 / 424 | N | In lab | N | N | - |
| [13] | Single | mesoporous 1D photonic crystal | N (VOCs) | Y | 11 / 76 | N | In lab | N | Y (filt,Wnd&Norm) | ML |
| [14] | Multiple (5) | MOx[1] | N (Whisky) | Y | 6 / 349 | Y | In lab | N | Y (Norm) | ML |
| [15] | Multiple (56) | MOx[1], EC[3], NDIR[4], PID[5] | Y (Illegal drugs) | Y | 3 / >3000 | N | In lab | N | Y (Norm) | ML |
| [16] | Multiple (64− >52) | Carbon Nanotubes | N (drinks) | Y | 6 / 6 | Y | In situ | N | N | ML |
| [17] | Multiple (4) | EC[3] | Y (VOCs) | Y | 4 / 4 | Y | In situ | Y | Y (Norm) | - |
| **Ours** | **Multiple (64− >52)** | **Carbon Nanotubes** | **Y (VOCs)** | **Y** | **5 / 5** | **Y** | **In situ** | **Y** | **N** | **ML/DNN** |

[1] MOx: Metal Oxide Semiconductor. [2] QMB: Quartz MicroBalance. [3] EC: ElectroChemical. [4] NDIR: Non-Dispersive Infrared. [5] PID: PhotoIonization Detector.

among others. Contact with ammonia can cause severe skin and eye irritation and burns, with the potential for serious eye damage. Inhalation of ammonia vapours can irritate the nose, throat and lungs, resulting in coughing and difficulty breathing. In extreme cases, exposure to high concentrations of ammonia can cause pulmonary edema and be fatal. It has one of the lowest recommended risk thresholds among the substances tested, with a maximum TLV of 25ppm for and 8-hours work shift and a STEL of 35ppm. [21].

Bleach is a clear, slightly yellow or green liquid with a strong chlorine odour which, on contact with air, decomposes releasing chlorine gas. It has an odour threshold ranging from 0.2 to 0.4 ppm. It is commonly mixed with water and used as a household cleaner and disinfectant. It is also used in water treatment and purification. Chlorine released as a gas can cause severe irritation and burns to the skin and eyes on contact, potentially leading to severe eye damage. Inhalation of chlorine can irritate the nose, throat and lungs, leading to symptoms such as coughing and breathing difficulties. In cases of severe exposure, chlorine can cause pulmonary oedema and be fatal. Chlorine has particularly low recommended exposure thresholds among the substances tested. An average TLV of 0.5 ppm for an 8-hour working day and a STEL of 1 ppm are recommended [22], [23].

## III. RELATED WORK

Electronic noses have a wide range of applications in various fields. In the food industry, they can be used to monitor and control the quality of food products by detecting the presence of contaminants, spoilage, or adulteration. In environmental monitoring, e-noses can be deployed to detect and identify pollutants or hazardous gases in the air or water. They are also used in healthcare for diagnosing diseases through breath analysis or detecting volatile biomarkers associated with certain medical conditions. A series of works devoted to different applications of eNose technologies have been analysed.

van der Sar et al. [24] analyse part of the State-of-the-Art (SoA) of electronic nose (eNose) technologies applied to detecting the smell of lung disease. This study summarises the technical aspects of available eNose devices and the existing evidence for their clinical application in different lung diseases. Similarly, Nurputra et al. [9] focus on developing a tool using an eNose as breath analyser for fast COVID-19 screening. This development leverages the fact that exhaled human breath contains volatile organic compounds (VOCs), which result from various metabolic pathways, and can serve as non-invasive biomarkers for various respiratory diseases.

Borowik et al. [10] examine different procedures to obtain the best performance in wine deterioration data from a reduced set of sensors and using their transient responses. Additionally, Viciano et al. [11] proposed a new system for characterising essential oils based on low-cost sensor networks and machine learning techniques. They achieved high accuracy in determining essential oils used in cosmetics (perfumes and flavourings), food (condiments and flavouring), and pharmaceutical (flavouring) industries.

Haddad et al. [12] applied the eNose technology to differentiate between pleasant and unpleasant odours. The authors used a MOSES II eNose, based on metal-oxide sensors and quartz microbalance sensors, alongside Machine Learning (ML) techniques to train an artificial intelligence network (ANN). They compared the results obtained from 123 odours (76 for training and 43 for testing), with human-subjective responses obtained from a survey. In this particular instance, the odours substances were initially subjected to individual dilutions, with the objective of achieving perceptual iso-intense conditions. Ratings ranged from “very unpleasant” to “very pleasant” on a 31-step scale (from 0 to 30).

Brandt et al. [13] developed a eNose-based system with array sensors, using ML techniques (e.g. SVM) to detect harmful substances capable of promoting wildfires. Similarly, Alishba et al. [25] reviewed the state of the art, analysing different applications of eNose-based systems with array sensors and their physical configuration.

Zhang et al. [14] used an array of 5 MOx sensors and a set of 45 features to classify 6 types of whiskey. They applied 5 ML classification methods in three different studies: classification of whiskey brand, whiskey style identification (blended malt and single malt) and region identification. Lozano et al. [16] used the same device to classify different beverages. Finally, Noh et al. [15] developed a hybrid sensing system to analyse illegal drugs.

Portable commercial solutions are also available for the detection of hazardous gases. More advanced models allow for custom configuration, where the user can select sensors according to their needs. An example is the Ventis Pro 5

This article has been accepted for publication in IEEE Sensors Journal. This is the author's version which has not been fully edited and
content may change prior to final publication. Citation information: DOI 10.1109/JSEN.2025.3567576



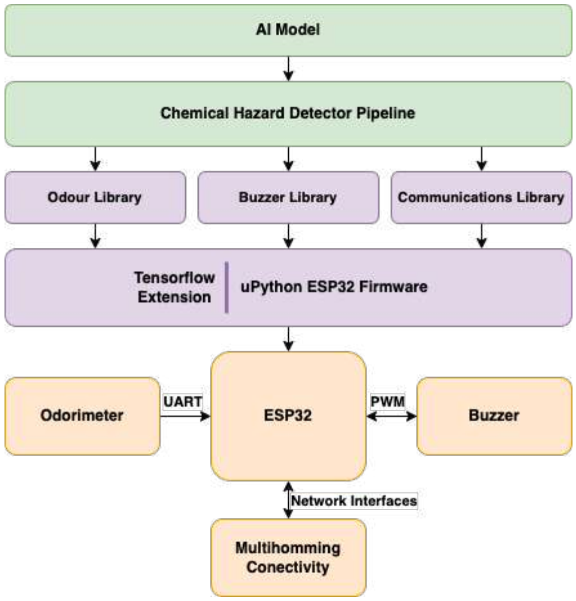


Fig. 1. System Architecture

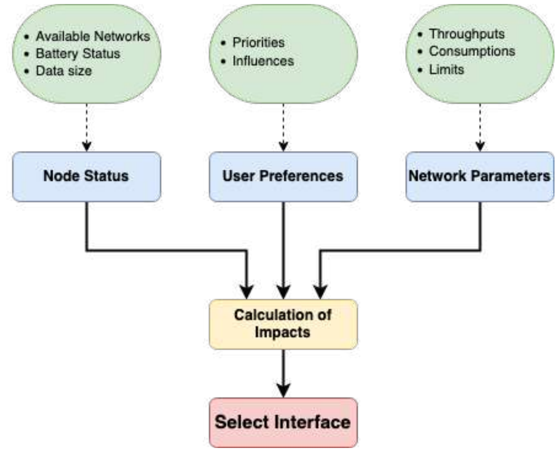


Fig. 2. Multihoming wireless technology selection Flow Chart

detector [17], which, in its standard configuration can detect carbon monoxide ($CO$), hydrogen sulphide ($H_2S$), oxygen ($O_2$) and an additional gas of the user's choice. Options for the latter include hydrogen cyanide ($HCN$), ammonia ($NH_3$), nitrogen dioxide ($NO_2$) and sulphur dioxide ($SO_2$). This model was selected in our study because it is the most economical in its category, allows ammonia detection and has WiFi and LTE communication capabilities, similar features to our proposed solution. The cost of this specific configuration with ammonia detection is £1,939.20 far above the £500 of our proposal which includes a fully integrated AI pipeline.

Table I shows a summary of the main features in the analysed SoA, demonstrating that our proposal technologically outperforms the existing state of the art.

## IV. System Architecture

Figure 1 shows the core component of the system, a microcontroller unit (MCU) Espressif ESP32-S3, known for its power and versatility in Internet of Things applications. This device is based on a 32-bit Xtensa LX7 CPU with a dual-core processor, operating at a frequency of up to 240 MHz. It is equipped with a 2.4 GHz Wi-Fi module and Bluetooth Low Energy (BLE), facilitating wireless connectivity. In addition, it has a wide variety of input and output interfaces, enabling integration with different sensors and actuators, thereby extending its capabilities for diverse applications.

This microcontroller is connected to an odorimeter via a UART interface. The odorimeter has 64 channels, each with different sensitivities, as well as integrated temperature and humidity sensors. Furthermore, it is designed for real-time operation, allowing for accurate and continuous monitoring.

Additionally, the system is equipped with a buzzer that emits acoustic signals to alert the user in case of positive detection. This feature provides an additional layer of interaction and security, ensuring that alerts are communicated immediately and effectively.

The system is also designed to enable connection to other network interfaces, beyond the already integrated WiFi and BLE in the ESP32, such as LoRa, LTE-M and other IoT technologies. This capability enables the implementation of multihoming algorithms, allowing for more robust and flexible communication across multiple networks. An implementation of these algorithms is found in Fayos et al. [26] for readers interested in further details.

The ESP32 has been programmed with our customized firmware that allows the execution of MicroPython code and has been modified to incorporate TensorFlow extensions. This adaptation was done following the guidelines described by Alselek et al. [27]. In summary, it allows TensorFlow Lite AI models to be updated while the device is in operation.

The system integrates a series of libraries developed specifically to control its different components. One of these libraries manages the buzzer, which emits warning sounds. The Odour library handles UART communications with the odorimeter, allowing real-time data collection. Finally, the communications library is responsible for selecting, through the multihoming algorithm, the best transmission route and sending the alerts to the cloud.

This algorithm, implemented in a MicroPython script, evaluates various communication options to select, combine or coordinate different wireless technologies, with the selection criteria depending on the location of the node, the available technologies, the available energy resources, and the IoT application itself as can be seen in Figure 2.

The throughput of each technology used, as well as the consumption per byte sent, has been measured empirically for Fipy boards and the results are documented in [26]. A concise summary is provided in Table IV.

The Chemical Hazard Detector Tiny-ML Pipeline loads the pre-trained AI model at the beginning of the process. This component is responsible for detecting hazardous chemicals based on the data provided by the odorimeter library. In case of a positive detection of a substance, it triggers the buzzer to emit a warning sound and sends a notification to the server. This notification includes the device identifier associated with the user, the detected substance, the date and time of the

This article has been accepted for publication in IEEE Sensors Journal. This is the author's version which has not been fully edited and content may change prior to final publication. Citation information: DOI 10.1109/JSEN.2025.3567576



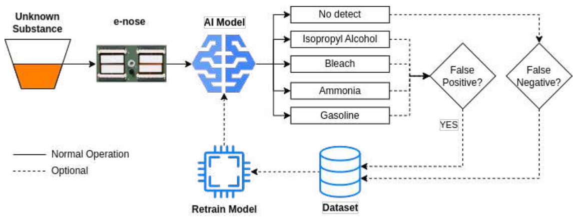


Fig. 3. Detector working

detection, and the data collected by the odorimeter. This data is stored so that, in the event of a false positive, it can be used to retrain and improve the AI model.

The AI model has previously been trained in controlled laboratory environments using the same odorimeter model. During this process, the model was exposed to a variety of chemicals to develop and validate its classification capabilities.

The system is able to operate anywhere on either battery or mains power, due to its low power consumption. It allows for the detection of a hazardous substance and the transmission of remote alerts via different wireless technologies (e.g. WiFi, LoRa, Bluetooth, or LTE-M).

Figure 3 shows the inference pipeline, where the system is exposed to an unknown substance, and the AI model infers the type of substance along with a confidence level. In the event of false positives or negatives, the model has the capacity to utilise the recorded data for the purpose of retraining, with a view to achieving enhanced accuracy.

## V. Tiny-ML Chemical Hazard Detection Pipeline

### A. Dataset

For the creation of the dataset, a connection was established between the odorimeter and a PC using the UART interface, along with a UART-USB converter. Using a Python script, all the data captured by the sensor was recorded and stored in a CSV file. To avoid possible interferences from other odours during the process, data collection was performed in a controlled environment, using a modified 5.4- liter container, as detailed in figure 4. A sample of the substance to be analysed was placed inside the container, while the top lid was adapted to house the odorimeter, ensuring that only the sensors were exposed to the substance. This setup prevented the sensors from detecting elements from the surrounding environment and ensured that the odorimeter was consistently exposed to the substance being measured. As a result, we obtained a gas mixture formed inside the container, consisting of the initial air and the vapours emitted by the substance. This evaporation at ambient temperature gradually saturated the gas, allowing the sensor to register different levels of exposure to the substance.

First, data collection was performed without the presence of any substance, in order to obtain a control sample of the air inside the container. Subsequently, data recording was conducted for each individual substance, ensuring that the container was thoroughly cleaned and ventilated before each measurement to prevent residual influence of the previously analysed substance on the new measurements.

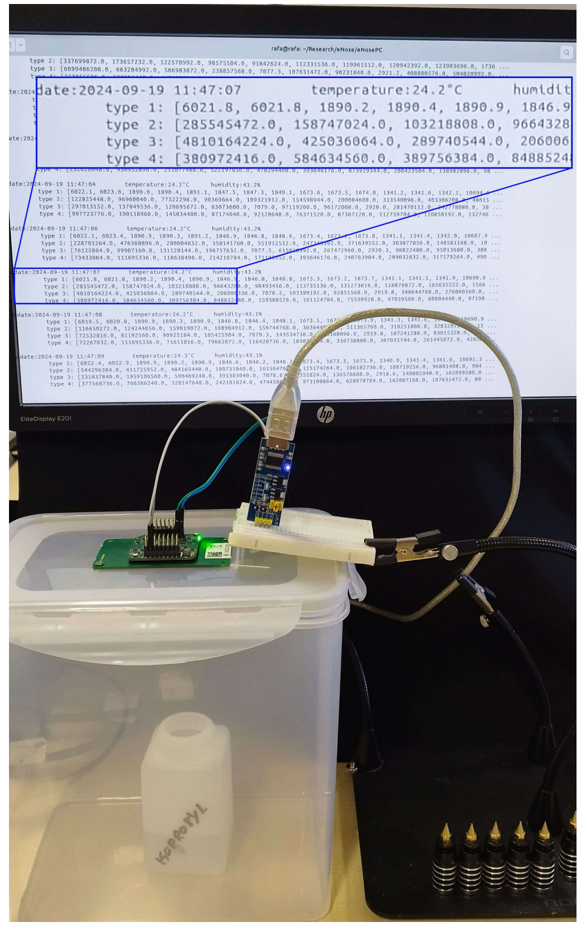


Fig. 4. Learning Process

The odorimeter measurements consists of 64-channel resistance value cycles, along with temperature and humidity values [28]. The 64 channels are made up of various types of feature channels, each with distinct smell sensitivity characteristics. Each detector contains 16 channels, and each channel represents a different set of characteristics. The current detectors include various feature set types, such as Type 1, Type 2, Type 3, and Type 4. Of the 64 available channels in the odorimeter, 19 provide only base resistance values and can therefore be omitted for substance detection. However, the recorded data of these channels were retained in case they prove to be relevant for future applications.

For each substance, a total of 2500 measurements were taken, at a rate of approximately one sample per second, resulting in a data collection period of just over 40 minutes per substance, ensuring a balanced dataset. Each data set has been stored in a CSV file, with each record including the date and time, temperature, humidity and the values corresponding to the 64 channels captured by the odorimeter. This system facilitates the tagging of the samples, as each file contains all the values of a single tag.

The substances analysed, as mentioned above, were bleach, ammonia, gasoline, isopropyl alcohol, and air, the latter used as a reference sample.

This article has been accepted for publication in IEEE Sensors Journal. This is the author's version which has not been fully edited and content may change prior to final publication. Citation information: DOI 10.1109/JSEN.2025.3567576



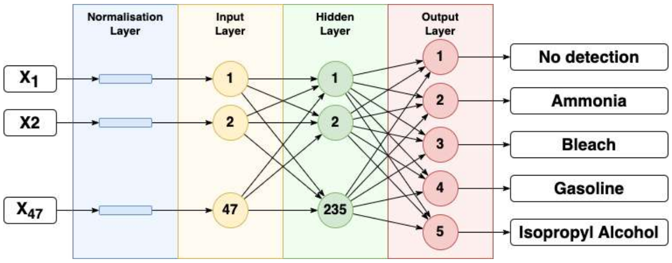


Fig. 5. Deep Neural Network design

### B. AI Model

For the design of a Tiny-ML model suitable for MicroPython, a simple MLP (Multilayer Perceptron) network has been selected due to its high effectiveness in performing classification tasks. This model has been implemented specifically for multi-class classification, using the TensorFlow library and the Keras API, tools that are widely recognised and commonly used in the development of deep learning models.

A normalisation layer has been incorporated into the model to standardise the input features. This layer shifts and scale inputs into a distribution centered around 0 with a standard deviation of 1. This adjustment enhances both the stability and performance of the model during the training process.

The input layer consist of 47 neurons, as illustrated in Figure 5. These neurons correspond to the values obtained from the multiple channels of the odometer, excluding the 19 channels that exclusively record base resistance values. Additionally, the input layer incorporates temperature and humidity values. A linear activation function has been applied in this layer.

The second layer consists of 235 fully connected neurons and uses the ReLU (Rectified Linear Unit) activation function, which introduces non-linearity into the model and enables it to learn more complex data representations. The number of neurons was determined through extensive testing, considering various approaches, such as the average between input and output neurons and the geometric pyramid rule [29], which involves the square root of the scalar product. Among other tested configurations to determine the number of neurons, it was observed that 235 neurons (the Cartesian product of 47 inputs and 5 different substances to detect) provided the highest accuracy. During experimentations, different options raging from 100 to 340 neurons, with increments of 15, were tested. The maximum accuracy was observed at 220 neurons, with a decline starting at 265. Increasing the number of neurons beyond this point did not yield additional accuracy improvements; therefore, the final configuration of 235 neurons was selected.

The final layer is a dense layer containing 5 neurons, each corresponding to one of the four analysed substances and to the absence of them. The softmax activation function has been applied to ensure that the network's output represents a probability distribution over the different classes.

The Adam optimiser was selected for its computational efficiency in TinyML environments, making it a suitable choice for the wearable device, which has limited hardware resources. The default learning rate value of 0.001 was also utilised. Adam's capability to manage adaptive gradients makes it a particularly suitable choice for this type of application.

### C. Training Pipeline

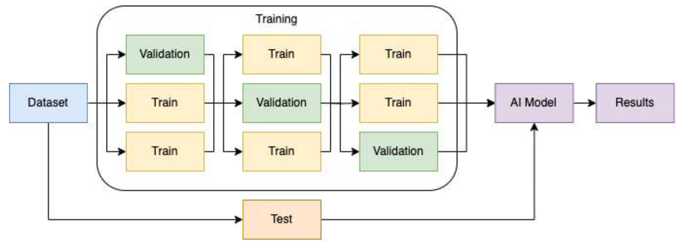


Fig. 6. Kfold Training and Test

For the training of the model, the dataset was divided into two subsets: a training set and a test set. Twenty per cent of the total samples were reserved for the test set, which is used to evaluate the final performance of the model after training is completed. The remaining 80% was used for training and validating the model. This process is illustrated in Figure 6

To ensure that the model does not overfit the training data and maintains generalization performance, the cross-validation technique was applied. In this case, the KFold function from the *sklearn* library was used, with a number of splits set to 3. KFold divides the training set into 3 distinct subsets. In each iteration, one of these subsets is used as the validation set, while the other two are combined to form the training set. This process is repeated 3 times, ensuring that each subset serves as the validation set once. This approach provides a more robust evaluation of the model and reduce the risk of overfitting.

Once the subsets were defined, the model was trained. This process was repeated for each iteration of cross-validation, resulting in three independent training runs. For each training subset, the model was trained for 15 epochs, with a batch size of 2. This approach allows the model to adjust its parameters more accurately and gradually, improving its ability to generalise to new data.

At the end of each epoch, the model's performance was evaluated using the validation subset. This monitoring process helps to detect potential problems such as overfitting. This approach ensures that the model not only fits the training data well, but also maintains good performance on new data.

Once the cross-validation process was completed, the model that demonstrated the best average performance across the validation subsets was selected. This model was then subjected to a final evaluation using the test set, which had not been used in any previous training phase.

This process was repeated for all the hidden layer configurations discussed in Section V-B to identify the most accurate configuration. Once the cross-validation process was complete, the model that achieved the best average performance among the validation subsets was selected. In this case, the model with 235 neurons in the hidden layer was chosen. This model was then subjected to a final evaluation using the test set, which had not been used in any previous training phase.

This article has been accepted for publication in IEEE Sensors Journal. This is the author's version which has not been fully edited and
content may change prior to final publication. Citation information: DOI 10.1109/JSEN.2025.3567576



## VI. Training Results

The results obtained during the training, validation and final testing of the model, as well as the analysis of its performance in terms of accuracy, loss and error distribution observed through the confusion matrix are presented in this section.

The model was trained using a 3-split K-Fold. In the first split, a remarkable instability was observed in the initial batches of the training. Specifically, the accuracy in batch 1 of 15 was 99.14%, while the corresponding loss was 7%. Over successive batches, the model's performance improved considerably, reaching an accuracy of 99.98% in batch 15 and reducing the loss to 2.4%, as shown in Figures 7 and 8. The loss function used was cross-entropy loss between true labels and predicted labels.

In comparison, splits 2 and 3 showed a higher stability from the initial batches. In both splits, the accuracy stabilised at 100%, while the loss remained close to 0% throughout the entire training process, demonstrating proper model convergence on these datasets.

Regarding validation, a trend similar to that observed during training was noted. In split 1, the validation accuracy started at 99.58% in batch 1 and reached 99.93% in batch 15. The loss, on the other hand, started at 3% and decreased to 1.4% by the end of the split. This initial instability in the first split may be due to insufficient adjustment in the early stages of training, which was progressively corrected.

For splits 2 and 3, the model consistently showed high performance in the validation. The accuracy stabilised at 99.98% in both splits, while the loss remained at 0.8% in split 2 and approached 0% in split 3, confirming the robustness of the model once it stabilised.

Finally, the model was evaluated using a test set consisting of 20% of the data, that was not used for training or validation. The results showed an accuracy of 99.96% and a loss of 1.14%, suggesting model's strong generalisation ability and performance on previously unseen data.

The confusion matrix obtained for the test set, with dimensions 5x5, is shown in table II.

TABLE II
CONFUSION MATRIX.

| | air | isopropyl | bleach | ammonia | gasoline |
|---|---|---|---|---|---|
| **air** | 472 | 0 | 0 | 0 | 0 |
| **isopropyl** | 0 | 503 | 0 | 0 | 0 |
| **bleach** | 0 | 1 | 531 | 0 | 0 |
| **ammonia** | 0 | 0 | 0 | 496 | 0 |
| **gasoline** | 0 | 0 | 0 | 0 | 498 |

The analysis of the confusion matrix reveals that the model correctly classifies the vast majority of instances in each of the five classes, with only one misclassification error. In particular, one instance of bleach was misclassified as belonging to isopropyl alcohol. This minimal error does not significantly affect the overall performance of the model, as the classification metrics show outstanding performance.

From the confusion matrix, precision, recall, and F1-score metrics have been calculated for each of the substances analysed. The results obtained are summarised in table III.

TABLE III
AI VALIDATION METRICS.

| | Precision | Recall | F1-Score | Support |
|---|---|---|---|---|
| **air** | 1.0000 | 1.0000 | 1.0000 | 472 |
| **isopropyl** | 0.9980 | 1.0000 | 0.9990 | 503 |
| **bleach** | 1.0000 | 0.9981 | 0.9991 | 532 |
| **ammonia** | 1.0000 | 1.0000 | 1.0000 | 496 |
| **gasoline** | 1.0000 | 1.0000 | 1.0000 | 498 |
| **Overall Accuracy** | 0.9996 | | | |

The model shows precision and recall close to 100% in all classes. In particular, the weighted average F1-score is 0.9996, which reflects the efficiency of the model in classifying instances, even in the case of a small error in one of the classes.

In summary, the trained model achieved a high level of accuracy and recall in both training and the final validation and test phases. Although slight instability was observed in the first batches of split 1, the model stabilised in the following splits and demonstrated robust and consistent performance, with an excellent ability to generalise to new data. The classification metrics and confusion matrix corroborate these findings, highlighting the model's effectiveness in the multi-class classification task.

## VII. Inference Results

The artificial intelligence model, initially developed in Keras, was 209 kB in size. To facilitate its implementation on a resource-constrained ESP32 device, it was converted to TensorFlow Lite, reducing its size to 62.8 kB. This optimisation represented a 69.96% decrease in the model's size, allowing it to run efficiently in environments with memory and processing capacity constraints.

The final device that houses the odorimeter has a power consumption profile that varies depending on the transmission mode and sensor activity. The average power consumption of the sensor, in isolation, is 104.2842 mW, with a minimum of 30 mW and peaks of up to 176 mW as shown in Figure 9. The total device consumption varies depending on the transmission technology used, as shown in table IV.

TABLE IV
POWER CONSUMPTION AND THROUGHPUT BY TRANSMISSION TECHNOLOGY.

| | WiFi | LTE | LoRa | BLE |
|---|---|---|---|---|
| **Consumption** | 1.5411 W | 1.2530 W | 1.6626 W | 1.4711 W |
| **Throughput** | 1800 kbps W | 50 kbps | 18 kbps | 18 kbps |

These variations in power consumption are key to selecting the most appropriate transmission method based on the device's operational needs and power constraints.

The average inference time of the model was 63.21 ms, with a standard deviation of 0.72 ms, as observed in Figure 10. These results demonstrate that the model is capable of real-time predictions (specifically, providing predictions at 15 Hz), offering sufficiently low latency for applications that require fast and efficient responses. This ensures adequate


(a)

Fig. 7. Accuracy training, validation and test. We used K-fold cross-validation, ensuring that each split was trained and validated separately with 15 epoch

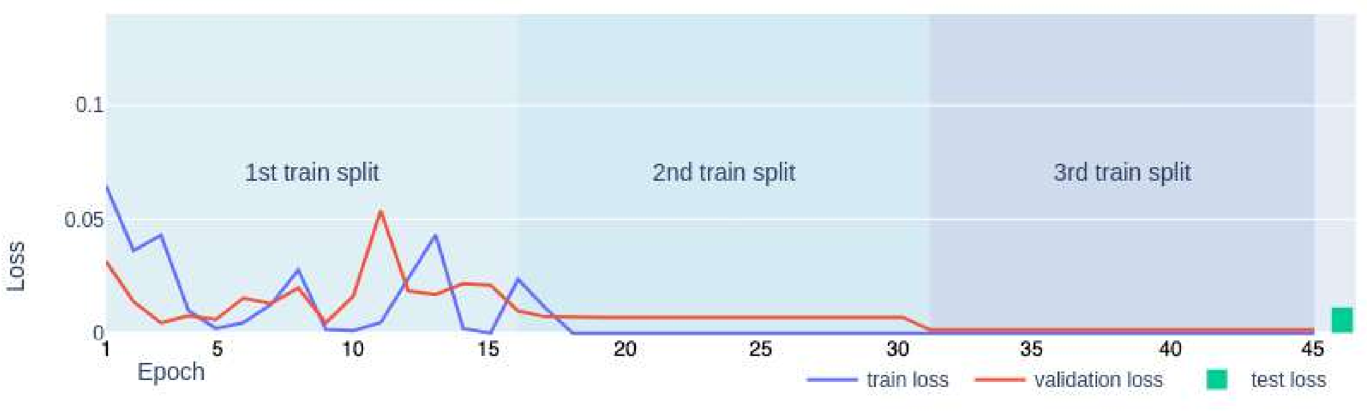


(a)

Fig. 8. Loss training, validation and test. We used K-fold cross-validation, ensuring that each split was trained and validated separately with 15 epoch

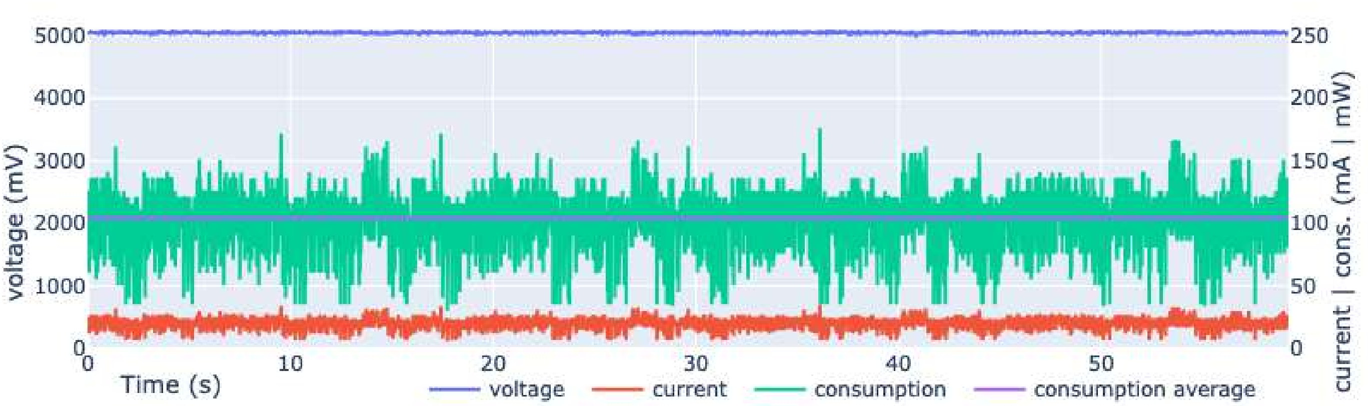


(a)

Fig. 9. E-nose power consumption

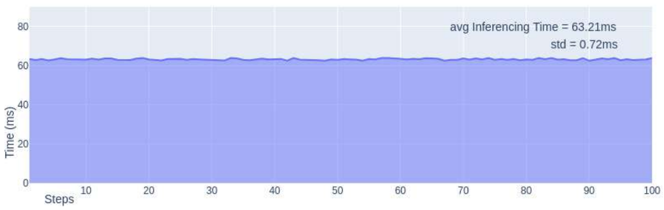


Fig. 10. Inferencing Times

performance in industrial environments, where time is crucial for worker safety.

Together, the optimised model, low power consumption, and reduced inference time ensure the efficient performance of the device and its artificial intelligence across various environments. These enhancements enable operation in applications with resource constraints, ensuring continuous and efficient functionality even under demanding conditions.

## VIII. System Validation

The aim of the system validation section is to evaluate the performance and effectiveness of a prototype IoT wearable device designed for the detection of hazardous substances. This device is equipped with TinyML capabilities, 5G LTE-M communications and an audio-visual alert system, which collectively make it a robust solution for industrial and security environments. Through a series of experiments conducted under controlled conditions, the device has been tested to ascertain its ability to detect different substances, issue alerts and record the information on a remote server.

The prototype is based on the Pycom FiPy development board, which incorporates an Espressif ESP32 SoC dual-core microcontroller and multiple communication interfaces, including LTE-M, WiFi, Bluetooth and LoRa. These communication channels are utilized to transmit the detected information.

As illustrated in Figure 11, an odorimeter has been connected to the device via UART for the purpose of measuring hazardous substances. Furthermore, an audible alert system has been implemented using a PWM-controlled buzzer, which emits sounds when a hazardous substance is detected. Additionally, the integrated LED is utilized for visual alerts.

The experiments have been conducted in a controlled environment, emulating industrially relevant scenarios in which various hazardous substances are released into the environment. A total of four distinct substances were selected, corresponding to the elements that the machine learning model was trained to identify. Three tests were conducted for each substance, resulting in a total of 12 experiments.

Each test involved exposing the device to the substance in question, followed by an examination of the device's ability to detect it and emit the corresponding alerts in the shortest possible time, as illustrated in Figure 12.

For the purposes of this experiment, the target substance was first placed within an airtight container, which was then placed on a table (75 cm in height) and subsequently on the floor. These two locations correspond to the most common

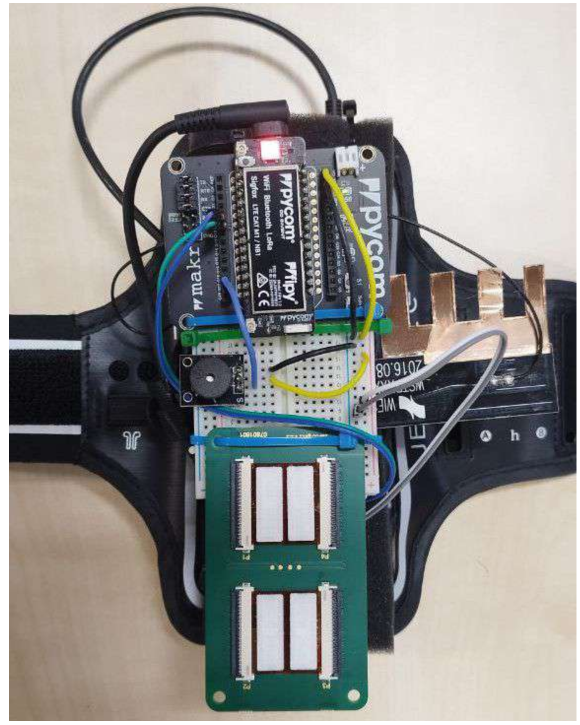

Fig. 11. Wearable Prototype

places in industry where accidents with hazardous substances occur and where workers are usually positioned. No other locations were considered, because the primary function of the device is to ensure immediate detection in the workplace for each worker equipped with one of these devices. In the subsequent stage, an individual equipped with a full Cat III protective suit, a gas mask, and goggles, with our prototype affixed to the arm (approximately 1.5 m in height), opened the container, thereby releasing the fumes of the substance. Concurrently, another individual commences a stopwatch. The experiment lasted for five seconds prior to the closure of the airtight container once more. However, in all cases, the device detected the substance in a significantly shorter timeframe and immediately commenced the emission of audio-visual signals as a consequence of the detection of a hazardous substance. The time elapsed from release to detection and from detection to registration in the database was meticulously documented.

Between each test, rigorous measures were implemented to prevent any cross-contamination of odours. The laboratory was ventilated between tests to guarantee that any residue from a previous substance did not affect the subsequent measurement.

The process validates not only the accuracy of the detection, but also the device's ability to communicate effectively with the server and record the information in real time.

In all tests conducted, the device performed as expected, correctly detecting the hazardous substance in all 12 experiments, giving a 100% success rate. Each time a substance was detected, the device provided both visual and audible alerts, ensuring an immediate response in the experimental environment. The time from vapour release to detection was approximately 1.2 seconds in all tests, and no significant differences were observed between the two positions tested. The


Fig. 12. In-Lab Test where Prof Jose M Alcaraz Calero (author) acts as operator to be exposed to a hazard substance wearing the prototype, in this case, being exposed to ammonia

LTE-M system was effective in transmitting data to the server, accurately recording the odorimeter readings and information corresponding to the substance detected. The average delay between the alert being registered in the IoT device and the alert being stored in a remote database is approximately 51ms.

## IX. Conclusion

This work has developed and validated an innovative system for detecting of hazardous substances, based on an IoT wearable prototype with TinyML capabilities, using a specially trained artificial intelligence model. The results obtained, both at the hardware and software levels, have been highly satisfactory, achieving the objectives set in terms of accuracy, energy efficiency and communication capacity and delivering a potential impact to enhance the safety of humans being exposed to hazardous substances.

Firstly, a new odour dataset has been created, which is not only useful for detecting hazardous substances, but also is extensible. Thanks to the use of a nanotube-based odorimeter, this dataset can be easily expanded to include more substances and adapt to the needs of different industries. This flexible approach allows for both the accurate detection of substances specific to a particular environment and the general detection of a larger number of substances, broadening the scope of the system.

Secondly, an artificial intelligence algorithm based on neural networks has been developed using a 4-layer multilayer perceptron. This model has shown remarkable reliability, achieving an accuracy of 99.98% in identifying the substances present in the dataset. The results show high stability, both in the training phase and in the validation and testing experiments. This confirms the high performance of the model and highlights its potential for applications in industrial or safety-critical scenarios.

In addition, the wearable prototype developed is presented as an advanced IoT solution, with TinyML capabilities, enabling real-time detection at a rate of 15 times per second with ultra-low power consumption. This makes it a highly efficient tool, not only for its ability to alert the wearer and nearby people via audio and visual signals, but also for its ability to send data to a central server via 5G, allowing for remote monitoring. This integration of technologies such as TinyML and 5G positions the device as a robust, versatile, and efficient solution for real-time hazard detection.

Finally, the prototype was tested in a relevant environment, demonstrating both its good performance and its practical utility. The correct identification of hazardous substances in various experimental situations, along with its alerting and data transmission capabilities, supports its effectiveness in real-life scenarios. This reinforces the feasibility of its implementation in industrial applications, where worker and environment safety can be significantly improved thanks to this system.

Although our system has been validated in controlled laboratory conditions, we acknowledge that real-world industrial environments present additional challenges such as background VOCs, fluctuating airflow, and higher noise levels. These factors may influence sensor performance and classification accuracy. Nevertheless, the device has been engineered to undertake training with the target substances in situ in industrial environments. Prior to deployment in any industry, the odourimeter must be exposed to the hazardous substances to be detected in the workplace. The training and resulting model should already take into account the background VOCs and correctly ignore them.

One of the most important conclusions of this work is the positive impact it can have on human safety. The development of a device capable of rapidly detecting hazardous substances and alerting those nearby has the potential to save many lives by reducing the risk of exposure in workplaces or in emergency situations. This technological breakthrough not only helps protect workers in hazardous industries, but also plays a crucial role in disaster mitigation.

In summary, the work has resulted in a smart wearable device that combines accurate hazardous substance detection, low power consumption and advanced connectivity with a highly reliable AI model. This development paves the way for future research and improvements in the detection of a wider range of substances, as well as its application in industries with specific safety needs, making a significant contribution to saving lives and protecting people in hazardous environments.

For future work, we plan to extend the number of detectable substances and enhance performance by exploring other types of neural networks and other microcontroller units (MCUs), such as Kendrite K210, Murata or equivalent, with higher PSRAM.

## Acknowledgment

The authors would like to thank to UKRI EPSRC EP/Y028813/1 ”National Edge AI Hub for Real Data: Edge Intelligence for Cyberdisturbances and Data Quality”. Also the EU Horizon P2CODE (”Programming Platform for Intelligent Collaborative Deployments over Heterogeneous Edge-IoT Environments”) project under the Grant number HORIZON-

CL4-2022-DATA-01-03/101093069. Also the Ministry of Science and Innovation for the project with number PID2021-126823OB-I00 and within the project Agriculture 6.0 with number TED2021-131040B-C33. Also, thank to the Generalitat Valenciana for the grant CIBEST/2023/101.

## REFERENCES


[1] F. Röck, N. Barsan, and U. Weimar, "Electronic nose: Current status and future trends," *Chem. Rev.*, vol. 108, p. 705–725, 2008.

[2] J. W. Gardner and P. N. Bartlett, "A brief history of electronic noses," *Sensors and Actuators B: Chemical*, vol. 18, no. 1, pp. 210–211, 1994. [Online]. Available: https://www.sciencedirect.com/science/article/pii/0925400594870853

[3] Word Health Organitation. Chemical safety. [Online]. Available: https://www.who.int/europe/news-room/fact-sheets/item/chemical--safety

[4] European Agency for Safety and Health at Work. Report - The practical prevention of risks from dangerous substances at work — Safety and health at work EU-OSHA. [Online]. Available: https://osha.europa.eu/en/publications/report-practical-prevention-risks-dangerous-substances-work

[5] Occupational Safety and Health Administration. Severe Injury Reports. [Online]. Available: https://www.osha.gov/severeinjury

[6] Gas Monitor Point. Honeywell BW™ Ultra 5 Gas Monitor. Gas Monitor Point. [Online]. Available: https://gasmonitor-point.co.uk/products/portable-gas-detectors/honeywell-bw-ultra-5-gas-monitor/

[7] ——. BW Clip4 Disposable Multi Gas Detector. Gas Monitor Point. [Online]. Available: https://gasmonitor-point.co.uk/products/portable-gas-detectors/bw-clip4-disposable-multi-gas-detector/

[8] ——. Blackline G7c Multi Gas Monitor LEL/O2/CO/H2S. Gas Monitor Point. [Online]. Available: https://gasmonitor-point.co.uk/products/portable-gas-detectors/blackline-g7c-multi-gas-monitor-lel-o2-co-h2s/

[9] D. K. Nurputra, A. Kusumaatmaja, M. S. Hakim, S. N. Hidayat, T. Julian, B. Sumanto, Y. Mahendradhata, A. M. I. Saktiawati, H. S. Wasisto, and K. Triyana, "Fast and noninvasive electronic nose for sniffing out covid-19 based on exhaled breath-print recognition," *npj Digital Medicine*, vol. 5, p. 115, 2022.

[10] P. Borowik, L. Adamowicz, R. Tarakowski, K. Siwek, and T. Grzywacz, "Odor detection using an e-nose with a reduced sensor array," *Sensors*, p. 3542, 2020.

[11] S. Viciano-Tudela, L. Parra, P. Navarro-Garcia, S. Sendra, and J. Lloret, "Proposal of a new system for essential oil classification based on low-cost gas sensor and machine learning techniques," *Sensors*, p. 5812, 2023.

[12] R. Haddad, A. Medhanie, Y. Roth, D. Harel, and N. Sobel, "Predicting Odor Pleasantness with an Electronic Nose," *PLOS Computational Biology*, vol. 6, no. 4, pp. 1–11, 04 2010. [Online]. Available: https://doi.org/10.1371/journal.pcbi.1000740

[13] S. Brandt, I. Pavlichenko, A. V. Shneidman, H. Patel, A. Tripp, T. S. B. Wong, S. Lazaro, E. Thompson, A. Maltz, T. Storwick, H. Beggs, K. Szendrei-Temesi, B. V. Lotsch, C. N. Kaplan, C. W. Visser, M. P. Brenner, V. N. Murthy, and J. Aizenberg, "Nonequilibrium sensing of volatile compounds using active and passive analyte delivery," *Proceedings of the National Academy of Sciences*, vol. 120, no. 31, p. e2303928120, 2023. [Online]. Available: https://www.pnas.org/doi/abs/10.1073/pnas.2303928120

[14] W. Zhang, T. Liu, A. Brown, M. Ueland, S. L. Forbes, and S. W. Su, "The Use of Electronic Nose for the Classification of Blended and Single Malt Scotch Whisky," *IEEE Sensors Journal*, vol. 22, no. 7, pp. 7015–7021, 2022.

[15] H. W. Noh, Y. Jang, H. D. Park, D. Kim, J. H. Choi, and C.-G. Ahn, "A selective feature optimized multi-sensor based e-nose system detecting illegal drugs validated in diverse laboratory conditions," *Sensors and Actuators B: Chemical*, vol. 390, p. 133965, 2023. [Online]. Available: https://www.sciencedirect.com/science/article/pii/S0925400523006809

[16] Á. Lozano Murciego, D. M. Jiménez-Bravo, G. Villarrubia González, A. Sales Mendes, and J. F. De Paz, "Smart electronic nose: An empirical evaluation of new multi-channel gas sensors for smell classification," in *New Trends in Disruptive Technologies, Tech Ethics and Artificial Intelligence*, D. H. de la Iglesia, J. F. de Paz Santana, and A. J. López Rivero, Eds. Cham: Springer Nature Switzerland, 2023, pp. 73–84.

[17] Industrial scientific ventis pro 5 (diffusion) multi-gas monitor (black) lens wireless. [Online]. Available: https://www.frontline-safety.co.uk/industrial-scientific-ventis-pro-5-diffusion-multi-gas-monitor-black-lens-wireless

[18] Agency for Toxic Substances and Disease Registry. Gasoline, Automotive — Medical Management Guidelines — Toxic Substance Portal — ATSDR. [Online]. Available: https://wwwn.cdc.gov/TSP/MMG/MMGDetails.aspx?mmgid=465&toxid=83

[19] New Jersey Department of Health. Gasoline Fact Sheet. [Online]. Available: https://nj.gov/health/eoh/rtkweb/documents/fs/0957.pdf

[20] ——. Isopropyl Alcohol Fact Sheet. [Online]. Available: https://nj.gov/health/eoh/rtkweb/documents/fs/1076.pdf

[21] ——. Ammonia Fact Sheet. [Online]. Available: https://nj.gov/health/eoh/rtkweb/documents/fs/0084.pdf

[22] ——. Sodium Hypochlorite Fact Sheet. [Online]. Available: https://nj.gov/health/eoh/rtkweb/documents/fs/1707.pdf

[23] ——. Chlorine Fact Sheet. [Online]. Available: https://nj.gov/health/eoh/rtkweb/documents/fs/0367.pdf

[24] I. G. van der Sar, N. Wijbenga, G. Nakshbandi, J. G. J. V. Aerts, M. S. W. O. C. Manintveld, M. E. Hellemons, and C. C. Moor, "The smell of lung disease: a review of the current status of electronic nose technology," *Respiratory Research*, vol. 22, p. 246, 2021.

[25] A. T. John, K. Murugappan, D. R. Nisbet, and A. Tricoli, "An outlook of recent advances in chemiresistive sensor-based electronic nose systems for food quality and environmental monitoring," *Sensors*, vol. 21, no. 7, 2021. [Online]. Available: https://www.mdpi.com/1424-8220/21/7/2271

[26] R. Fayos-Jordan, S. Felici-Castell, J. Segura-Garcia, J. M. Alcaraz-Calero, and A. Cervello-Duato, "Exploiting multihoming capabilities in 5g-enabled IoT nodes," *IEEE Access*, vol. 11, pp. 134 940–134 950, 2023. [Online]. Available: https://ieeexplore.ieee.org/document/10336763/

[27] M. AlSelek, J. M. Alcaraz-Calero, and Q. Wang, "Dynamic AI-IoT: Enabling Updatable AI Models in Ultralow-Power 5G IoT Devices," *IEEE Internet of Things Journal*, vol. 11, no. 8, pp. 14 192–14 205, 04 2024. [Online]. Available: https://ieeexplore.ieee.org/document/10349697

[28] SmartNanotubes Technologies GmbH. Technical Manual Smell Board. [Online]. Available: https://smart-nanotubes.com/wp-content/uploads/2024/04/SNT_Manual_Smell_Board_V1.2.0.pdf

[29] Timothy Masters, *Practical Neural Network Recipes in C++*. Morgan Kaufmann, 1993.


**Rafael Fayos-Jordan** BSc Hons, MSc and Ph.D. in Information Technologies, Communications and Computing from the University of Valencia. Research Assistant at University of the West of Scotland

**Mohammad Alselek** Ph.D. from University of the West of Scotland. Assistant Professor at the University of the West of Scotland, UK,

**Mohammad Khadmaoui-Bichouna** Ph.D. from The University of the West of Scotland, BSc Hons in Telecommunications Engineering from the University of Valladolid. ML Engineer at Tech Lead

**Jaume Segura-Garcia** M.Sc. and Ph.D. degrees in physics from the University of Valencia. Associate Professor at the Department of Computer Science, University of Valencia.

**Jose M. Alcaraz-Calero** PhD, MEng, SMIEEE & FHEA. Full Professor in Next-Generation Cyber Security at Aston Univerity.

**Qi Wang** Ph.D. degree in mobile networking from the University of Plymouth. Full Professor with the University of the West of Scotland.